Journal of Chemical Technology and Metallurgy, 53, 5, 2018, 845-855

DISSOLUTION KINETICS STUDIES OF NIGERIAN GYPSUM ORE IN HYDROCHLORIC ACID

Folahan Amao Adekola, Adebayo Isaac Olosho,
Alafara Abdullahi Baba, Samad A. Adebayo

Department of Industrial Chemistry
University of Ilorin
Ilorin, Nigeria
E-mail: adebayoolosho@gmail.com
fadekola@unilorin.edu.ng

Received 15 November 2017
Accepted 30 May 2018

ABSTRACT

Dissolution kinetics studies of gypsum ore sourced from Postikum, Northern Nigeria, was conducted using hydrochloric acid as the leachant. The study was done with the aim of establishing possibility for the development of hydrometallurgical route for the production of highly pure gypsum. The effects of the experimental variables investigated were contact time, acid concentration, temperature, particle size and solid-liquid ratio. The energy of activation of the dissolution reaction estimated from experimental data is 9.6 kJ mol^{-1}. Leaching in 6 M HCl solution, at temperature of 80^{o}C, stirring speed of 400 rpm and using – 90 + 63 μm particle size resulted in 99.7 % dissolution of the ore within 120 min. The ore and the leached residue were characterised using X-ray Fluorescence (XRF), X-ray Diffraction (XRD), and Scanning Electron Microscope (SEM) coupled with energy dispersive spectroscopy techniques (EDS) for chemical composition, phase and morphology. Statistical analysis of the kinetic dissolution data shows that the chemical controlled model best describes the gypsum dissolution in hydrochloric acid.

Keywords: gypsum ore, hydrochloric acid, dissolution kinetics, chemical controlled model.

INTRODUCTION

Gypsum is a sedimentary rock, an evaporited mineral formed as precipitate when sea water evaporates [1]. It is naturally found with some impurities which include limestone, red shale, marl, clays, halite, celestine, calcite, aragonite, anhydrite, dolomite and magnesian [2].

There are two molecules of water chemically bound with calcium sulphate. Heating the mineral at temperature between 100^{o}C - 170^{o}C, causes it to lose one-third of its water of crystallization to form hemihydrates ($CaSO_4.½\ H_2O$), which is also called plaster. Plaster of Paris can easily be converted back to gypsum in the presence water liberating heat and forming a hard cast which set in 5 - 20 minutes [3]. The chemistry of these processes can be summarised in equation (1)

$$CaSO_4.2H_2O \underset{\text{Setting and Hardening}}{\overset{120\text{-}200^0C}{\rightleftharpoons}} \underset{\text{Plaster}}{CaSO_4.\tfrac{1}{2}H_2O + 1\tfrac{1}{2}H_2O} \xrightarrow{\text{Above } 200^0C} CaSO_4 + 1\tfrac{1}{2}H_2O \quad (1)$$

This property makes gypsum a very useful as a casting material in the field of orthopaedic surgery, interior designs for building and cement production.

The Nigerian Ministry of Solid Minerals Development reported that there are about one billion tonnes of gypsum deposit across the country, spread over places like Nafada/Bajoga in Gombe State, Fika in Yobe State,

Guyuk/Gwalura in Adamawa State and Igankoto in Ogun State [1]. Despite the abundance of gypsum and other material needed for the production of Plaster of Paris (POP) in the country, the country relies heavily on the importation of these products.

The solubility of gypsum in different media has been studied extensively. Most kinetics studies of gypsum dissolution in water revealed that dissolution rate is controlled by a reaction on the surface of the mineral [4]. The study of solubility of calcium sulphate dihydrate, hemihydrate, and anhydrite in concentrated HCl, $CaCl_2$ and their mixed aqueous solution using classic isothermal dissolution method has been done by Li and Demopoulos [5]. It was reported that the solubility of $CaSO_4$ phases increases with concentration and temperature. The solubility of gypsum in other media such as H_2SO_4/manganese sulphate media and in ternary systems of $CaSO_4 + MSO_4 + H_2O$ through isothermal solution saturation at 348.1 K and 363.1 K was also studied. Cobalt and Nickel were the metals used [6, 7]. However, previous work on the study of leaching kinetics of gypsum, especially in HCl media, and the quantitative purification of the mineral in the acid media, was not found.

In the leaching of minerals, different oxidizing reagents are used as the leaching medium, these reagents include hydrochloric acid, sulfuric acid, nitric acid and other oxidizing agents [8]. Pure gypsum free of gangue is white and is a valuable compound for the production of Plaster of Paris used for orthopaedic surgery and plasterboards.

The aim of this study is to establish the physico-chemical condition for the leaching of Nigerian gypsum ore by hydrochloric acid, which can be used to predict possible condition for the production of highly pure gypsum.

EXPERIMENTAL

The gypsum ore sample used for this research was obtained from a gypsum quarry site in Potiskum, Yobe State, Nigeria. The sample was pulverized and sieved to produce four particle size fractions: - 90 + 63 μm, - 112 + 90 μm, - 180 + 112 μm and - 250 + 180 μm using ASTM standard sieves. All experiments were performed with particle size fraction of - 90 + 63 μm unless otherwise stated. The characterization of gypsum ore before and after leaching at optimal conditions were carried out using EDX3600B Skyray X-ray fluorescence, GBC enhanced mini-materials analyser (eMMA) X-ray diffraction and Leo 1450 Scanning electron microscopy. Chemie Lobal analytical grade Hydrochloric acid and distilled water were used in the preparation of all solutions

Leaching Procedure

This procedure was carried out in a 1L glass reactor equipped with a magnetic stirrer [9]. The reactor filled with the 500 ml of 0.2 M HCl and heated to 80°C. 5 g of the gypsum ore was introduced into the reactor and covered with a glass lid. The solution was stirred at the rate of 400 rpm with the aid of the magnetic stirrer for various contact time of 10, 30, 60 and 120 minutes. At the end of each period, the solution was cooled and filtered. The residue was washed with distilled water and oven dried at about 55°C for one hour and weighed to obtain the fraction of gypsum dissolved. The same procedure was repeated for 0.5 M, 1.0 M, 2.0 M 4.0 M and 6.0 M, respectively. The concentration that yielded the maximum dissolution was subsequently used for the optimization of other leaching parameters such as gypsum ore particle size (- 90 + 63 μm, - 112 + 90 μm, - 180 + 112 μm and - 250 + 180 μm), solid-liquid ratio (10 g/L, 20 g/L and 40 g/L) and reaction temperature of 32 to 80°C [8, 10]. The residue obtained was characterized with XRD and SEM-EDS.

RESULTS AND DISCUSSION

Chemical Analysis by X-Ray Fluorescence

The chemical composition of the gypsum ore sample, obtained by X-ray Fluorescence, are expressed as oxides, mass %. The major oxides detected are calcium (46.23 mass %), sulphur (50.48 mass %), aluminium (1.62 mass %), silicon (1.25 mass %) and iron (0.369 mass %) oxide. The quantity of manganese oxide found was at trace level. This result is similar to those reported by Irahbor et al., and López-Delgado et al. [1, 11].

Phase Characterisation with X-Ray Diffraction

The gypsum ore X-ray diffraction pattern is shown in Fig. 1. The diffraction revealed that the ore is rich in gypsum complementing the result of the chemical analysis by X-Ray Fluorescence. The phases were identified using the Joint Committee on Powder Diffraction

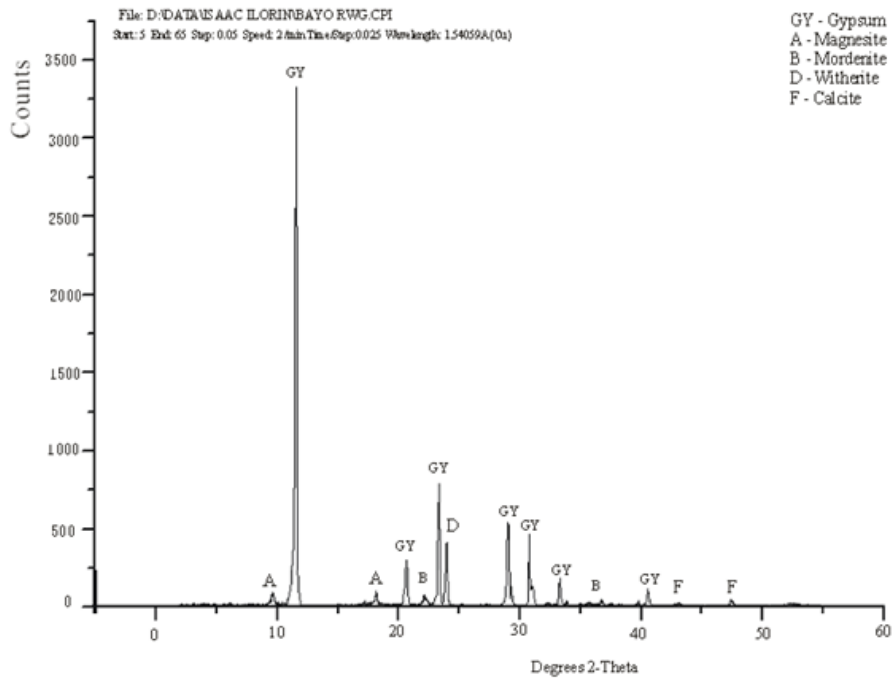

Fig. 1. XRD pattern of the gypsum ore sample showing different phases present with respective JCPDS file number used for peak attribution GY- Gypsum (01-070-0982), A-Magnesite (36-0383), B-Mordenite (49-0924), D- Witherite (5-0378), and F-Calcite (5-0586).

Standard File number. The compound present in the ore include: Gypsum (01-070-0982), Magnesite (36-0383), Mordenite (49-0924), Witherite (5-0378), and Calcite (5-0586). Other minor phases that occurred in low to trace levels include Anatase (21-1272) and Chrysotile (25-0645) [11 - 13].

Morphological Characterization of Gypsum Ore

The microstructure, surface morphology and elemental percentage composition of raw gypsum ore (RWG) was characterized with Scanning Electron Microscopy-Energy Dispersive Spectroscopy (SEM-EDS). The equipment model is Leo 1450 with LaB_6 filament. The samples were viewed at 200 X and 1.0 KX magnification, 13 mm working distance and were carbon coated. The element analysis was done with a Brinker X-Flash detector using Esprit 1.82 software. The micrographs at both magnifications are given in Fig. 2. The image in Fig. 2a shows particles of different topography, while some seems to be homogeneous with

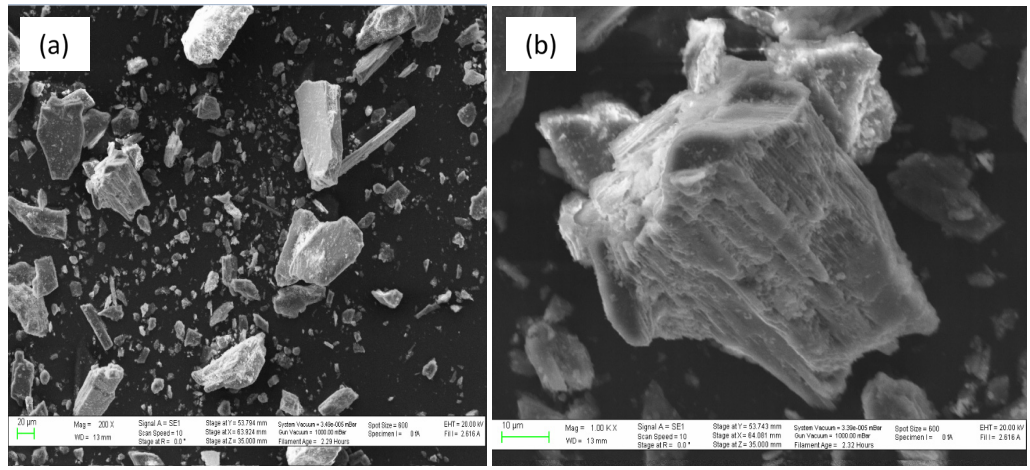

Fig. 2. Micrograph of raw gypsum ore (RWG) at (a) 200 x magnification; (b) 1.0 Kx magnification.

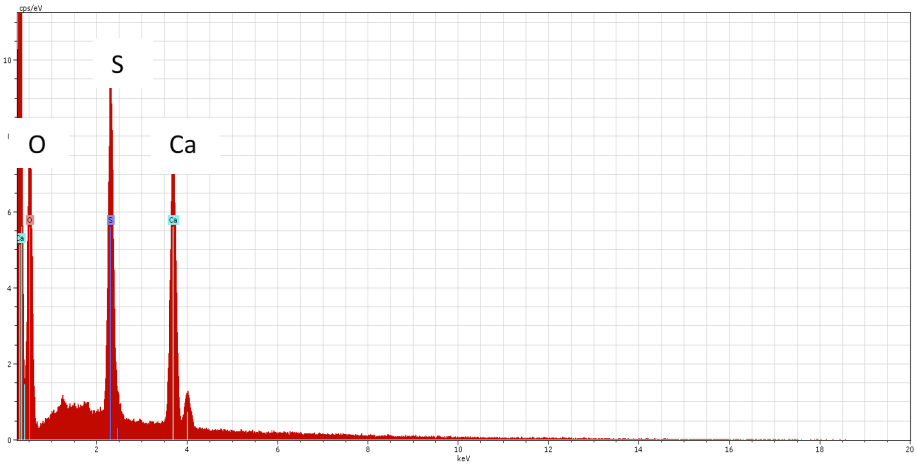

Fig. 3. Electron Dispersive Spectroscopy Spectrum of raw gypsum ore (RWG).

few deposits of different phases on their surfaces others consist entirely of heterogeneous phase. At a higher magnification of 1.0 KX, the image in Fig. 2b shows clearly that the particle is a conglomerate deposition of different constituents. These imply that RWG is a heterogeneous material consisting of different phases (compounds). This supports the result obtained by X-ray diffractometer where other phases such as calcite, whiterite, modernite and others were identified.

The spectrum of the elemental analysis by Energy Dispersive Spectroscopy in Fig. 3 shows that calcium, sulphur and oxygen are the most abundant elements in RWG. This is in consonance with that of X-ray Fluorescence and phase identification of X-ray Diffraction. From the aforementioned characterisation, it can be concluded that RWG is indeed gypsum ore with impurities present. These impurities are what is responsible for brown colour and will impair the effectiveness of the material if directly used without purification.

Results of Dissolution Studies

Effect of Acid Concentration

The effect of acid concentration was studied in the range of 0.2 M - 6.0 M acid concentration at 80°C using - 90 + 63 μm particle size with a stirring speed of 400 rpm. The fraction dissolved is plotted against leaching time for the different concentration of the acid as shown in Fig. 4. The results indicated that gypsum rapidly dissolves up to about 96 % in a short time even at concentration as low as 0.2 M. A significant increase in

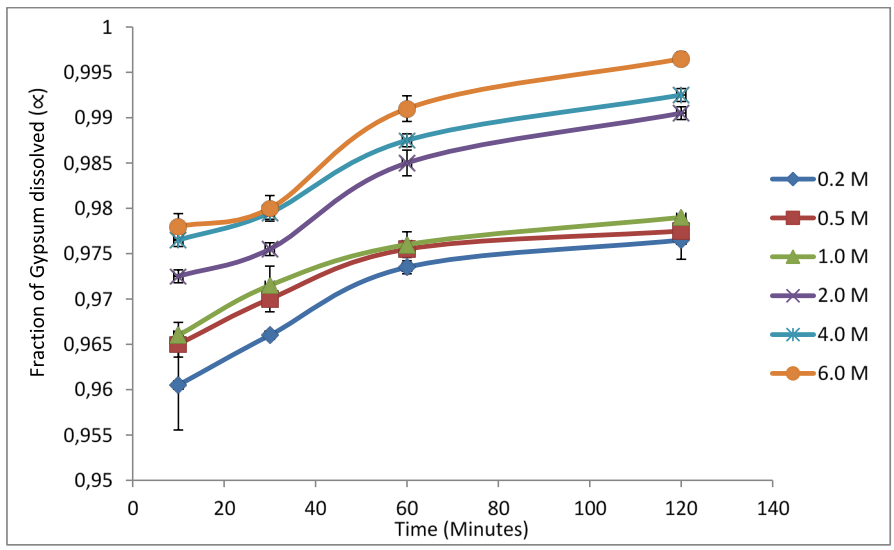

Fig. 4. Plot of fraction of gypsum dissolved versus leaching time at different concentrations of HCl. (Experimental conditions: solid-liquid ration: 10 g/l; stirring rate: 400 rpm; particle size: - 90 + 63 μm; temperature: 80°C).

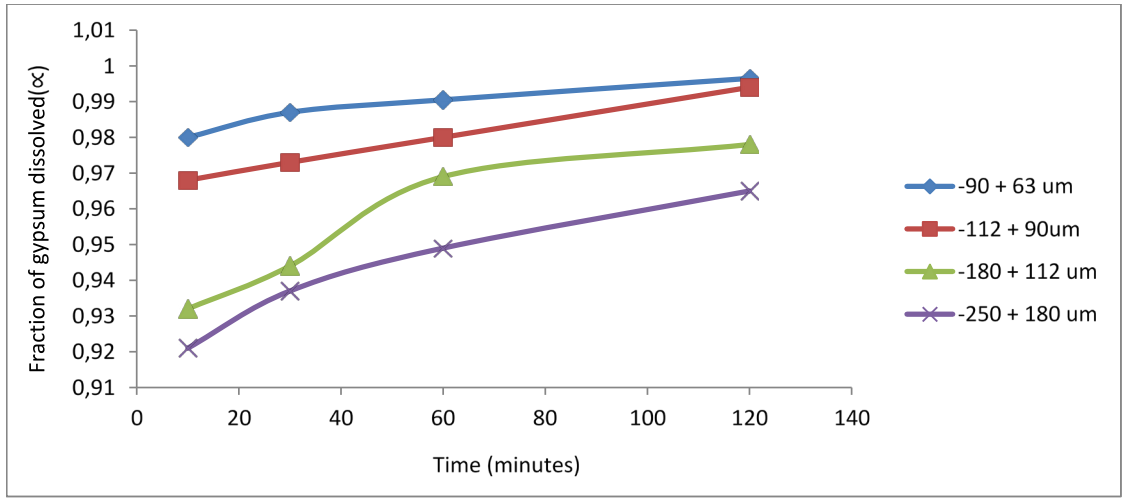

Fig. 5. Plot of fraction of gypsum dissolved versus leaching time at different particle sizes. (Experimental conditions: solid-liquid ration: 10 g/l; stirring rate: 400 rpm; [HCl] = 6.0 M; temperature: 80°C).

dissolution was observed between 1.0 M and 2.0 M concentration of the acid. The leaching rate further increased with increase in acid concentration to a maximum of 99.7 %. This result indicates that gypsum dissolution is controlled by the hydrogen ion [H^+] concentration in the solution. This agrees with earlier studies on mineral ores [14, 15]. As indicated in the plot, error margin was computed over a range of three values for each point on the plot.

Effect of Particle Size

The effect of particle size on the rate of gypsum dissolution in hydrochloric acid was studied over the range of four particle sizes: - 90 + 63 µm, - 112 + 90 µm, - 180 + 112 µm, and - 250 + 180 µm. Fig. 5 gives a graphical impression of the effect. It was observed that the rate decreases with increase in particle size because an increase in surface area will give rise to a higher reaction rate as the solution portions are made more accessible to the solvent. In addition to the importance of size reduction, the surface area per unit weight of the sample increases causing greater amount of gypsum to be liberated from the matrix of the raw gypsum rock [10]. This supports earlier reports that dissolution rate is inversely proportional to average initial diameter particles [16]. The fraction of gypsum dissolved increased with increase in contact time for all particle size fractions.

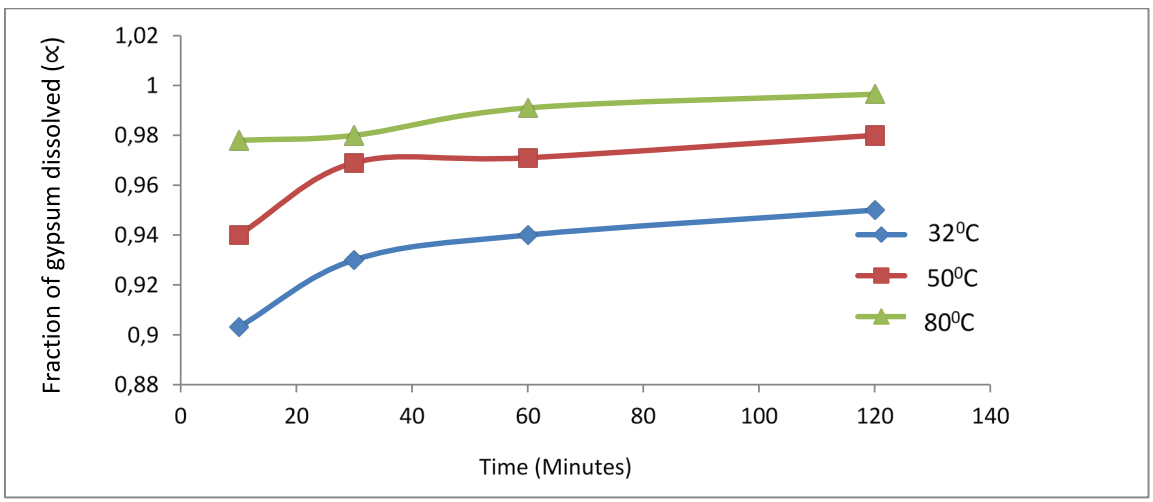

Fig. 6. Plot of fraction of gypsum dissolved versus leaching time at different temperatures. (Experimental conditions: solid-liquid ration: 10 g/l; stirring rate: 400 rpm; particle size: - 90 + 63 µm; [HCl] = 6.0 M).

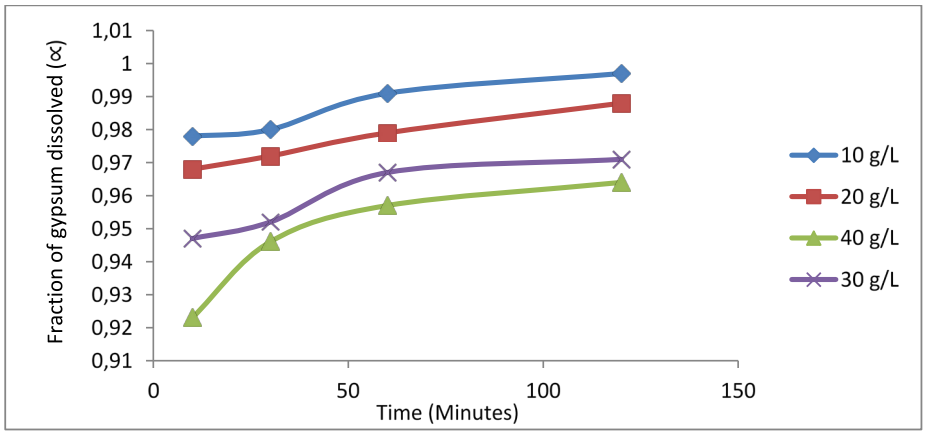

Fig. 7. Plot of fraction of gypsum dissolved versus leaching time at different solid-liquid ratio. (Experimental conditions: particle size: -90 + 63 μm; [HCl] = 6.0 M; temperature 32°C).

Effect of Temperature

A number of experiments were also conducted to study the effect of temperature on the dissolution rate of gypsum in HCl acid. The reaction conditions are as follows: [HCl] = 6.0 M at 80°C using - 90 + 63 μm particle size with a stirring speed of 400 rpm. Fig. 6 gives the graphical representation. The results indicate that dissolution rate increases with an increasing of temperature. The maximum dissolution of 99.7 % was obtained at 80°C. This is similar to reports from other studies on kinetic leaching of ore in acid media [17, 18].

Effect of Solid-Liquid Ratio

The effect of different solid-liquid ratio was studied in a number of experiments over a range of 10 - 40 g/L. At experimental conditions of - 90 + 63 μm gypsum particle size; 6.0 M hydrochloric acid solution and temperature of 80°C. The summary of the results is given in Fig. 7. As expected, quantity of gypsum ore dissolved decreased as the solid-liquid ratio increase [17].

Analysis of Dissolution kinetics by Shrinking Core Models

The shrinking core model is always applied to describe the leaching kinetics where there is a reduction in both the mass and the particle size of the solid during leaching [8]. The overall reaction for dissolution of gypsum by hydrochloric acid may be written as follows:

$$CaSO_4.2H_2O + 2HCl_{(aq)} \rightarrow CaCl_{2(aq)} +$$

$$+ H_2SO_{4(aq)} + H_2O_{(l)} \quad (2)$$

For the dissolution kinetics of gypsum by HCl, the three established kinetic models were tested with all the experimental data expressed in Figs. 4 - 7. These are diffusion, chemical and mixed controlled kinetic models. If the reaction rate is controlled by diffusion through the product layer, chemically or by both (mixed), integrated rate equation (3), (4) or (5) holds, respectively.

$$1 - \frac{2}{3}(1-\alpha)^{\frac{2}{3}} = \frac{2MDC}{\beta\rho r_0^2}t = K_d t \quad (3)$$

$$1 - (1-\alpha)^{\frac{1}{3}} = \frac{kC}{r_0\rho}t = K_c t \quad (4)$$

$$1 - (1-\alpha)^{\frac{1}{3}} + \frac{y}{6}\left[(1-\alpha)^{\frac{1}{3}} + 1 - 2(1-\alpha)\right]^{\frac{2}{3}} = K_m t \quad (5)$$

In equations (3 - 5), K_d, K_c and K_m are the rate constants for diffusion, chemical and mixed controlled leaching, respectively. ∝, r_0, ρ, M, D, C and t are the fraction of the solid phase reacted, initial radius of the solid particle, density, molecular mass of the solid, diffusion coefficient in the porous product layer, concentration of the dissolved leachant and the reaction time, respectively [19].

These models were compared as shown in Table 1. Statistical analysis of the kinetic dissolution data shows that chemical controlled model best describes gypsum dissolution in hydrochloric acid.

According to the equation (4), a plot of $1-(1-\propto)^{\frac{1}{3}}$ vs. leaching time is a straight line with slope K_c when the process is diffusion controlled as shown in Fig. 8. The experimental rate constants K_c were evaluated from the

Table 1. Shrinking Core Model Comparison.

Parameters	Kinetic Models								
	Diffusion Control $1-\frac{2}{3}\propto-(1-\propto)^{\frac{2}{3}}$			Chemically Controlled $1-(1-\propto)^{\frac{1}{3}}$			Mixed Controlled $1-(1-\propto)^{\frac{1}{3}}+[\frac{1}{6}(1-\propto)^{\frac{1}{3}}+1-2(1-\propto)^{\frac{2}{3}}$		
		$k_d \times 10^{-4}$	R_d^2		$k_c \times 10^{-4}$	R_c^2		$k_m \times 10^{-4}$	R_m^2
Concentration (M)									
0.2		2.059	0.877		4.815	0.883		9.992	0.876
0.5		1.642	0.847		3.892	0.852		7.958	0.846
1.0		1.720	0.885		4.115	0.893		8.334	0.885
2.0		3.214	0.952		8.470	0.961		15.722	0.953
4.0		3.079	0.959		8.475	0.969		15.192	0.961
6.0		4.129	0.949		12.30	0.965		20.859	0.955
Order of Reaction	0.2		0.660	0.3		0.716	0.2		0.667
Temperature (^{0}C)									
32		3.548	0.821		3.548	0.828		18.183	0.812
50		3.985	0.726		3.985	0.749		19.489	0.722
80		4.129	0.949		4.128	0.965		20.859	0.955
Activation Energy	2.6 Kjmol^{-1}		0.847	9.6 kJ/mol		0.999			
Particle size									
-90 + 63 um		3.394	0.967		11.835	0.995		19.652	0.987
-112 + 90 um		4.620	0.993		12.490	0.985		22.788	0.992
-180 +112 um		3.392	0.937		7.573	0.945		16.621	0.934
-250 + 180 um		2.432	0.814		4.970	0.817		12.678	0.807
Plot of k_d Vs $1/r^2$			0.989						
Plot of k_d Vs $1/r$						0.913			
Solid-Liquid Ratio (g/L)									
10		4.309	0.958		13.015	0.973		21.880	0.964
20		6.893	0.916		14.148	0.923		36.378	0.900
40		12.88	0.998		27.145	0.993		85.042	0.981

slope of Fig. 8. The values were then used to plot ln K_c vs. ln[HCl] as shown in Fig. 9. The slope of Fig. 9 was calculated to be 0.3. This indicates that the reaction order with respect to HCl leaching for which its concentration is 6.0 M is 0.3. The chemical controlled model was also used to linearize Fig. 6. The linearity of the data is shown in Fig. 10. The apparent K_c were determined from the slopes of the straight lines in Fig. 10 and were used to plot Arrhenius plot of Fig. 11.

From the Arrhenius plot of Fig. 11, the activation energy was calculated to be 9.6 kJ mol^{-1}. This value suggests a diffusion controlled mechanism as against the chemically controlled mechanism from statistical analysis [8]. However, it has been argued that the rate controlling mechanism of heterogeneous dissolution reactions is better predicted from plots of the kinetic equations rather than from the activation energy value [16, 17].

The low value of activation energy also suggests that the reaction between gypsum and hydrochloric acid proceeds rapidly to product. This can be made evident in Figs. 4 - 7 where about 90 % gypsum ore reacts with the acid in ten minutes. The value further suggests also that dissolution of gypsum in hydrochloric acid at the given particle size fraction and acid concentration does not require large quantity of heat. The plot of K_c against the inverse of square of particle radii (1/r) gave a linear relationship as shown in Fig. 12. This further proves that the reaction is chemically controlled.

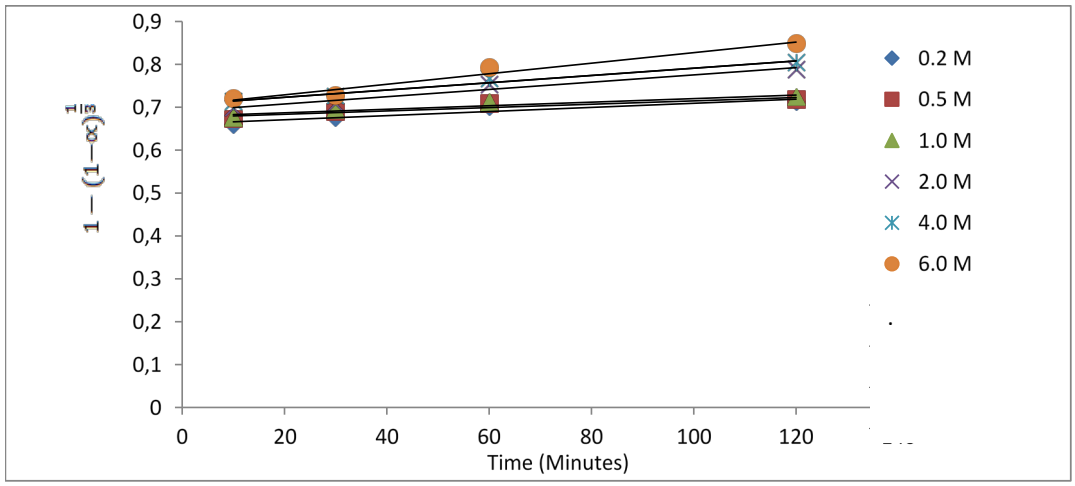

Fig. 8. Plot of $1-(1-\propto)^{\frac{1}{3}}$ vs. leaching time at different HCl concentration.

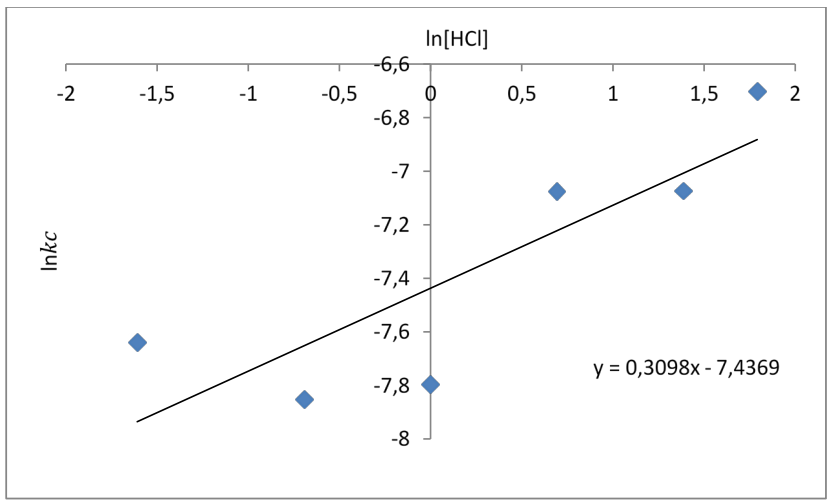

Fig. 9. Plot of ln K_c against ln[HCl].

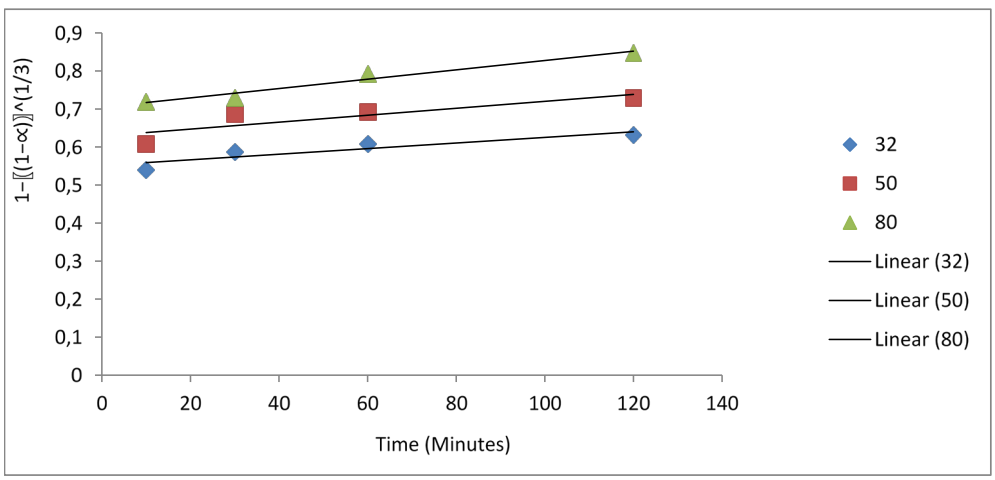

Fig. 10. Plot of $1-(1-\propto)^{\frac{1}{3}}$ vs. leaching time at different temperature.

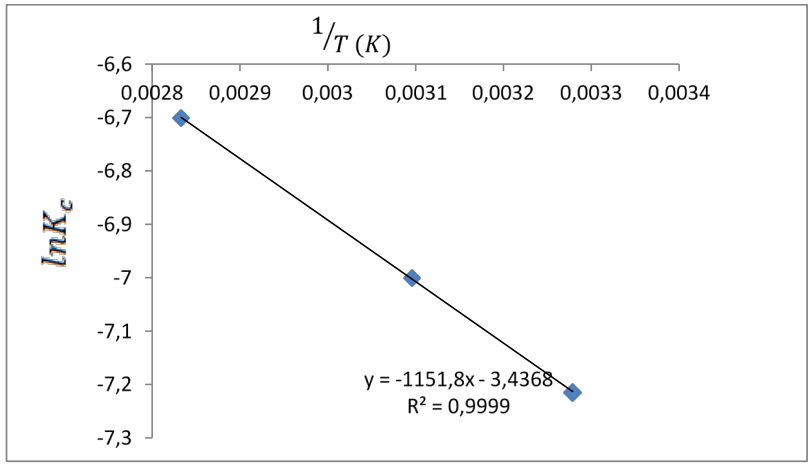

Fig. 11. Plot of ln K_c vs. $^1/_T\ (K^{-1})$.

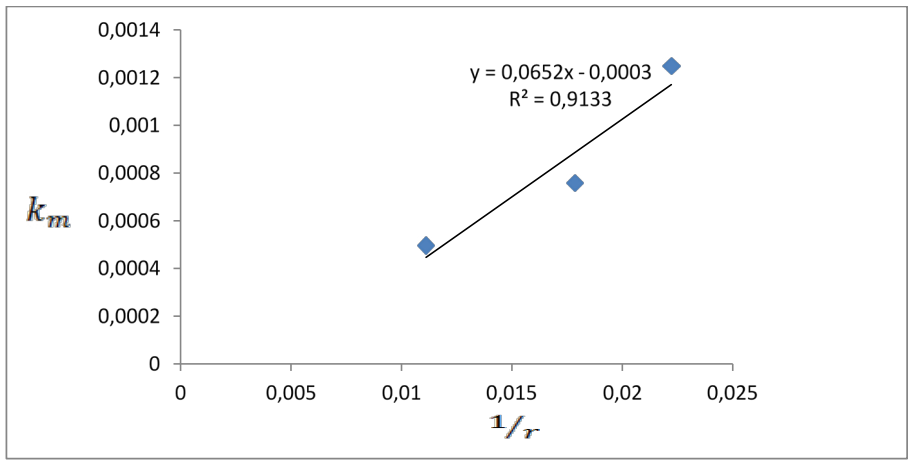

Fig. 12. Plot of K_m vs. (1/r).

Characterisation of Leached Residue from Dissolution Studies

The leached residue (LR) was analysed with GBC enhanced mini-materials analyzer (eMMA) X-ray Diffractometer. The solid residual products obtained from the leaching of 10 g/L gypsum ore at optimum condition of 6.0 M, 80°C, 400 rpm, superimposed with the raw gypsum (RWG) sample is presented in Fig. 14. It was observed that as at 6.0 M HCl concentration, gypsum had been completely leached as no gypsum phase was seen in the XRD pattern. The phases that are predominant in the leached residue include magnesite (36-0383), mordenite (49-0924), witherite (5-0378), anatase (21-1272) and quartz (46-1045) [11 - 13]. The phases found in the leached residue (Fig. 13) are the impurities in the raw sample with no trace of the gypsum phase. This implies that the compound of interest has been completely leached at the stated optimum condition. The microstructure, surface morphology and elemental percentage composition of the gypsum recovered from the hydrochloric acid leached liquor was also characterized with Leo 1450 Scanning Electron Microscopy with Energy Dispersive Spectroscopy (SEM-EDS). The micrographs at 200 x and 1.0 Kx magnifications are given in Fig. 14. The images show particles of similar topography with those of the raw sample in Fig. 2 suggesting that the leached residue is also heterogeneous in nature consisting of different phases. The spectrum of the elemental analysis by Energy Dispersive Spectroscopy in Fig. 15 shows that silicon, aluminium and iron are the abundant elements in the residue.

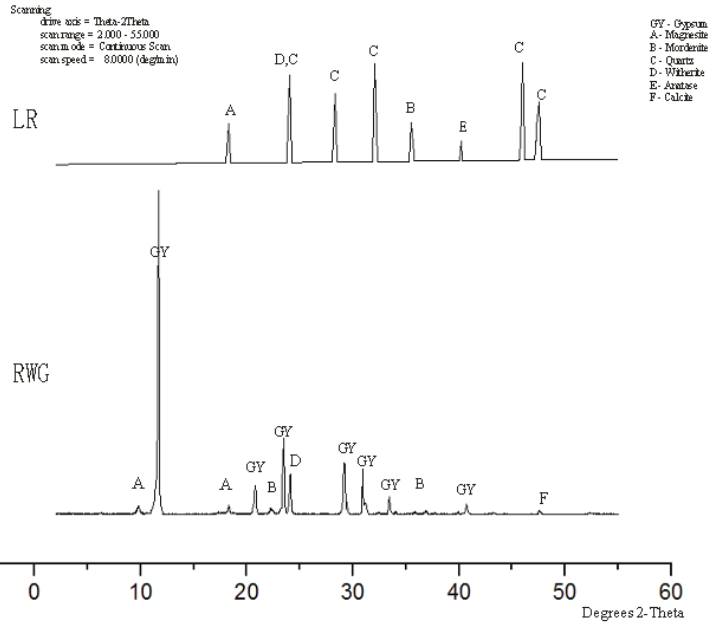

Fig. 13. XRD pattern of 10 g/L gypsum leached residue at 6.0 M HCl, 80°C, 400 rpm.

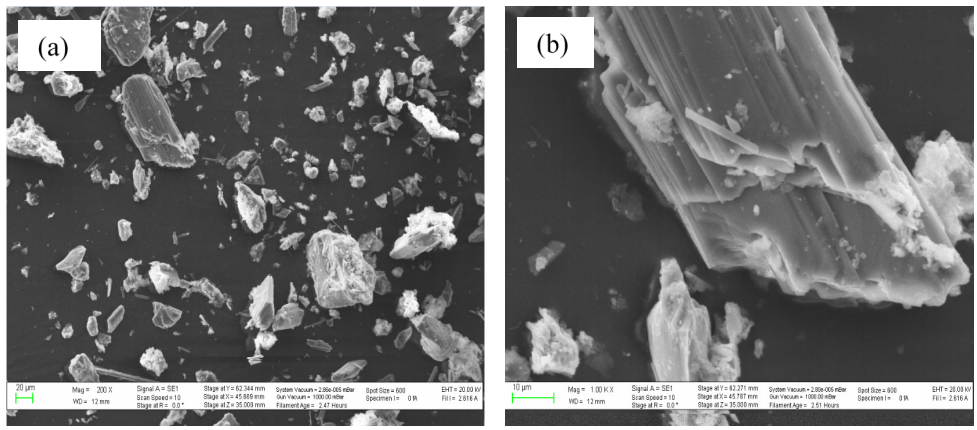

Fig. 14. Micrographs of leached residue at (a) 200 x and (b) 1.0 Kx magnifications.

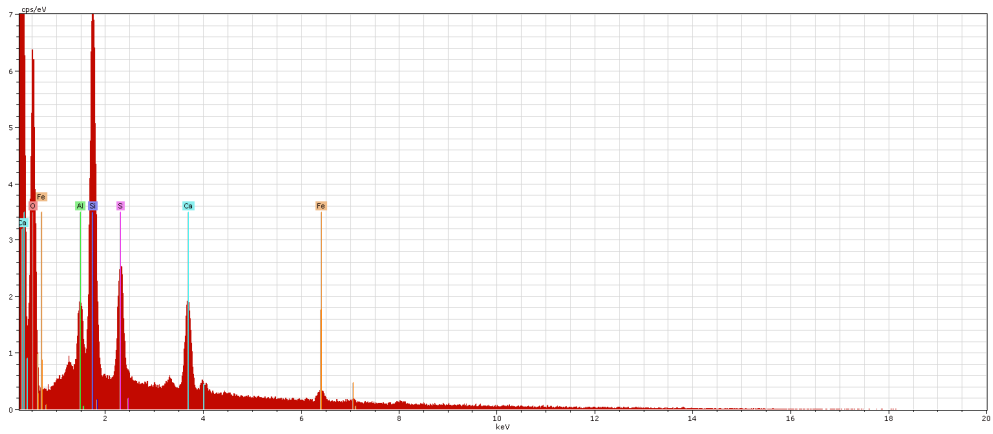

Fig. 15. Electron Dispersive Spectroscopy Spectrum of leached residue (LR).

CONCLUSIONS

This study examined the dissolution kinetics of gypsum ore in hydrochloric acid. The results obtained showed that the reaction rate increases with hydrogen ion [H^+] concentration, and reaction temperature but decreases with particle size and solid-liquid ratio. The shrinking core model that best described the dissolution kinetics was estimated to be chemically controlled model. The reaction order with respect to [H^+] ion concentration was found to be 0.3 and a value of 9.6 kJ/mol was obtained as energy of activation, Ea, for the dissolution process. The study also shows that gypsum ore readily dissolves in hydrochloric acid at low temperature making possible recovery of gypsum from the leached liquor a viable option.

REFERENCES

1. P.S.A. Irabor, S.O. Jimoh, O.J. Omowumi, B.S.O. Ighalo, Physical and chemical analysis of some Nigerian gypsum minerals for application in manufacturing, construction and allied industries, Int. J. Sci. Tech. Res., 2, 10, 2013, 229-235.
2. J.R. Gunn, Evolution in Gypsum Mining, Gypsum Journal, 49, 1968, 14-18.
3. M. Sayonara, M. Pinheiro, C. Gladis, Characteristics of gypsum recycling in different cycles, Int. J. Eng. Tech., 7, 3, 2015, 215-228.
4. A.L. Lebedev, Kinetics of gypsum dissolution in water, J. Geochem. Int., 53, 9, 2015, 811-824.
5. Z. Li, G.P. Demopoulos, Solubility of CaSO4 in Aqueous HCl + $CaCl_2$ Solutions from 283K to 353 K, J. Chem. Eng. Data, 50, 2005, 1971-1982.
6. H.E. Farrah, G.A. Lawrence, E.J. Wanless, Solubility of calcium sulphate salts in acid manganese sulphate solutions from 30 to 105^{o}C, Hydrometallurgy, 86, 1-2, 2007, 13-21.
7. W. Wang, D. Zeng, H. Zhou, X. Wu, X. Yin, Solubility Isotherms of Gypsum, Hemihydrate, and Anhydrite in the Ternary Systems CaSO4 + MSO4 + H2O (M = Mn, Co, Ni, Cu, Zn) at T = 298.1 K to 373.1 K, J. Chem. Eng. Data, 60, 10, 2015, 3024-3032.
8. A.A. Baba, I.A. Kuranga, B.B. Rafiu, F.A. Adekola, Quantitative Leaching of a Nigerian Chalcopyrite Ore by Nitric Acid, Bay. J. Pure Appl. Sci., 7, 2, 2014, 115- 121.
9. S. Aydogan, A. Aras, M. Cambazoglu, Dissolution kinetics of sphalerite in acidic ferric chloride leaching, Chem. Eng. J., 114, 2005, 67-72.
10. M. Gharabaghi, M. Irannajad, A.R. Azadmehr, Leaching kinetics of nickel extraction from hazardous waste sulphuric acid and optimisation dissolution conditions, Chem. Eng. Res. Des., 91, 2, 2013, 325-331.
11. A. López-Delgado, S. López-Andrés, I. Padilla, M. Alvarez, R. Galindo, A.J. Vázquez, Dehydration of gypsum rock by solar energy: preliminary study, J. Geomater., 4, 2014, 82-91.
12. A. Zelati, A. Ahmad, K. Ahmad, Preparation and Characterization of Barium Carbonate Nanoparticles, Int. J. Chem. Eng. Appl., 2, 4, 2011, 299-303.
13. P. Intarapong, S. Iangthanarata, P. Phanthonga, A. Luengnaruemitchaia, S. Jai-In, Activity and basic properties of KOH/mordenite for transesterification of palm oil, J. Energ. Chem., 22, 2013, 690-700.
14. E.O. Olanipekun Quantitative leaching of galena, Bull. Chem. Soc. Ethiopia, 14, 1, 2000, 25-32.
15. A.A. Baba, F.A. Adekola, A.O. Folashade, Quantitative leaching of a Nigerian Iron ore in hydrochloric acid, J. Appl. Sce. Environ. Mgt., 9, 1, 2005, 15-20.
16. E. Olanipekun, A kinetic study of the leaching of a Nigerian ilmenite ore by hydrochloric acid, Hydrometallurgy, 53, 1999, 1-10.
17. A.A. Baba, F.A. Adekola, R.B. Bale, Development of a combined pyro- and hydro-metallurgical route to treat spent zinc–carbon batteries, J. Hazard. Mater., 171, 2009, 838-844.
18. J. Li, J.D. Miller, Reaction kinetics of gold dissolution in acid thiourea solution using ferric sulphate as oxidant, Hydrometallurgy, 89, 3-4, 2007, 279-288.
19. O. Gerald, N. Christopher, O. Ayebatonvoio, O. Martin, Comparative kinetics of Iron Ore Dissolution in Aqueous HCl-HNO3 system, J. Miner. Mater. Characterization & Engineering, 1, 4, 2013, 153-159.